

1 **An infectious SARS-CoV-2 B.1.1.529 Omicron virus escapes neutralization by**
2 **several therapeutic monoclonal antibodies**

3
4 Laura A. VanBlargan¹, John M. Errico², Peter J. Halfmann³, Seth J. Zost^{4,5}, James E. Crowe
5 Jr.^{4,5,6}, Lisa A. Purcell⁷, Yoshihiro Kawaoka^{3,8,9}, Davide Corti¹⁰, Daved H. Fremont^{2,11,12}, and
6 Michael S. Diamond^{1,2,11,13,14}

7
8 ¹Department of Medicine, Washington University School of Medicine, St. Louis, MO, USA
9 ²Department of Pathology & Immunology, Washington University School of Medicine, St. Louis, MO,
10 USA
11 ³Influenza Research Institute, Department of Pathobiological Sciences, School of Veterinary Medicine,
12 University of Wisconsin-Madison, Madison, WI, USA.

13 ⁴Vanderbilt Vaccine Center, Vanderbilt University Medical Center, Nashville, TN, USA
14 ⁵Department of Pediatrics Vanderbilt University Medical Center, Nashville, TN, USA
15 ⁶Department of Pathology, and Microbiology and Immunology, Vanderbilt University Medical Center,
16 Nashville, TN, USA

17 ⁷Vir Biotechnology, St Louis, MO, USA.
18 ⁸Division of Virology, Department of Microbiology and Immunology, Institute of Medical Science,
19 University of Tokyo, 108-8639 Tokyo, Japan.

20 ⁹The Research Center for Global Viral Diseases, National Center for Global Health and Medicine
21 Research Institute, Tokyo 162-8655, Japan.

22 ¹⁰Humabs BioMed SA, a subsidiary of Vir Biotechnology, Bellinzona, Switzerland.
23 ¹¹Department of Molecular Microbiology, Washington University School of Medicine, St. Louis, MO.
24 ¹²Department of Biochemistry & Molecular Biophysics, Washington University School of Medicine, St.
25 Louis, MO.

26 ¹³Andrew M. and Jane M. Bursky Center for Human Immunology and Immunotherapy Programs,
27 Washington University School of Medicine, Saint Louis, MO.

28 ¹⁴Center for Vaccines and Immunity to Microbial Pathogens, Washington University School of Medicine,
29 Saint Louis, MO.

30 **Corresponding author:** Michael S. Diamond, M.D., Ph.D., mdiamond@wustl.edu

31 **ABSTRACT**

32 **Severe acute respiratory syndrome coronavirus 2 (SARS-CoV-2) has caused the**
33 **global COVID-19 pandemic resulting in millions of deaths worldwide. Despite the**
34 **development and deployment of highly effective antibody and vaccine countermeasures,**
35 **rapidly-spreading SARS-CoV-2 variants with mutations at key antigenic sites in the spike**
36 **protein jeopardize their efficacy. Indeed, the recent emergence of the highly-transmissible**
37 **B.1.1.529 Omicron variant is especially concerning because of the number of mutations,**
38 **deletions, and insertions in the spike protein. Here, using a panel of anti-receptor binding**
39 **domain (RBD) monoclonal antibodies (mAbs) corresponding to those with emergency use**
40 **authorization (EUA) or in advanced clinical development by Vir Biotechnology (S309, the**
41 **parent mAbs of VIR-7381), AstraZeneca (COV2-2196 and COV2-2130, the parent mAbs of**
42 **AZD8895 and AZD1061), Regeneron (REGN10933 and REGN10987), Lilly (LY-CoV555**
43 **and LY-CoV016), and Celltrion (CT-P59), we report the impact on neutralization of a**
44 **prevailing, infectious B.1.1.529 Omicron isolate compared to a historical WA1/2020 D614G**
45 **strain. Several highly neutralizing mAbs (LY-CoV555, LY-CoV016, REGN10933,**
46 **REGN10987, and CT-P59) completely lost inhibitory activity against B.1.1.529 virus in**
47 **both Vero-TMPRSS2 and Vero-hACE2-TMPRSS2 cells, whereas others were reduced**
48 **(~12-fold decrease, COV2-2196 and COV2-2130 combination) or minimally affected**
49 **(S309). Our results suggest that several, but not all, of the antibody products in clinical use**
50 **will lose efficacy against the B.1.1.529 Omicron variant and related strains.**

51 **MAIN TEXT**

52 Since December of 2019, the global COVID-19 pandemic caused by SARS-CoV-2 has
53 resulted in 267 million infections and 5.3 million deaths. The expansion of the COVID-19
54 pandemic and its accompanying morbidity, mortality, and destabilizing socioeconomic effects
55 have made the development and distribution of SARS-CoV-2 therapeutics and vaccines an
56 urgent global health priority¹. While the rapid deployment of countermeasures including
57 monoclonal antibodies and multiple highly effective vaccines has provided hope for curtailing
58 disease and ending the pandemic, this has been jeopardized by emergence of more transmissible
59 variants with mutations in the spike protein that also could evade protective immune responses.

60 Indeed, over the past year, several variant strains have emerged including B.1.1.7
61 (Alpha), B.1.351 (Beta), B.1.1.28 [also called P.1, Gamma]], and B.1.617.2 (Delta), among
62 others, each having varying numbers of substitutions in the N-terminal domain (NTD) and the
63 RBD of the SARS-CoV-2 spike. Cell-based assays with pseudoviruses or authentic SARS-CoV-
64 2 strains suggest that neutralization by many EUA mAbs might be diminished against some of
65 these variants, especially those containing mutations at positions L452, K477, and E484²⁻⁶.
66 Notwithstanding this, *in vivo* studies in animals showed that when most EUA mAbs were used in
67 combination they retained efficacy against different variants⁷. The recent emergence of
68 B.1.1.529, the Omicron variant^{8,9}, which has a larger number of mutations (~30 substitutions,
69 deletions, or insertions) in the spike protein, has raised concerns that this variant will escape
70 from protection conferred by vaccines and therapeutic mAbs.

71 We obtained an infectious clinical isolate of B.1.1.529 from a symptomatic individual in
72 the United States (hCoV-19/USA/WI-WSLH-221686/2021). We propagated the virus once in
73 Vero cells expressing transmembrane protease serine 2 (TMPRSS2) to prevent the emergence of

74 adventitious mutations at or near the furin cleavage site in the spike protein¹⁰. Our B.1.1.529
75 isolate encodes the following mutations in the spike protein (A67V, Δ69–70, T95I, G142D,
76 Δ143-145, Δ211, L212I, insertion 214EPE, G339D, S371L, S373P, S375F, K417N, N440K,
77 G446S, S477N, T478K, E484A, Q493R, G496S, Q498R, N501Y, Y505H, T547K, D614G,
78 H655Y, N679K, P681H, N764K, D796Y, N856K, Q954H, N969K, and L981F; **Fig 1a-b** and
79 GISAID: EPI_ISL_7263803), which is similar to strains identified in Africa¹¹. Our isolate,
80 however, lacks an R346K mutation, which is present in a minority (~8%) of reported strains.

81 Given the number of substitution in the B.1.1.529 spike protein, including eight amino
82 acid changes (K417N, G446S, S477N, Q493R, G496S, Q498R, N501Y, Y505H) in the ACE2
83 receptor binding motif (RBM), we first evaluated possible effects on the structurally-defined
84 binding epitopes of mAbs corresponding to those with EUA approval or in advanced clinical
85 development (S309 [parent of VIR-7381]^{12,13}; COV2-2196 and COV2-2130 [parent mAbs of
86 AZD8895 and AZD1061, respectively]¹⁴; REGN10933 and REGN10987¹⁵, LY-CoV555 and
87 LY-CoV016^{16,17}; and CT-P59 [Celltrion]¹⁸) along with an additional broadly neutralizing mAb
88 (SARS2-38) that we recently described¹⁹. We mapped the B.1.1.529 spike mutations onto the
89 antibody-bound SARS-CoV-2 spike or RBD structures published in the RCSB Protein Data
90 Bank (**Fig 1c-k**). While every antibody analyzed had structurally defined recognition sites that
91 were altered in the B.1.1.529 spike, the differences varied among mAbs with some showing
92 larger numbers of changed residues (**Fig 1l**: COV2-2196, n = 4; COV2-2130, n = 4; S309, n = 2;
93 REGN10987, n = 4; REGN10933, n = 8; Ly-CoV555, n = 2; Ly-CoV016, n = 6; CT-P59, n = 8;
94 and SARS2-38, n = 2).

95 To address the functional significance of the spike sequence variation in B.1.1.529 for
96 antibody neutralization, we used a high-throughput focus reduction neutralization test (FRNT)²⁰

97 with WA1/2020 D614G and B.1.1.529 in Vero-TMPRSS2 cells (**Fig 2**). We tested individual
98 and combinations of mAbs that target the RBD in Vero-TMPRSS2 cells including S309 (Vir
99 Biotechnology), COV2-2130/COV2-2196 (parent mAbs of AZD1061 and AZD8895 provided
100 by Vanderbilt University), REGN10933/REGN10987 (synthesized based on casirivimab and
101 imdevimab sequences from Regeneron), LY-CoV555/LY-CoV016 (synthesized based on
102 bamlanivimab and etesevimab sequences from Lilly), CT-P59 (synthesized based on
103 regdanvimab sequences from Celltrion), and SARS2-38. As expected, all individual or
104 combinations of mAbs tested neutralized the WA1/2020 D614G isolate with EC₅₀ values similar
105 to published data^{6,18,21}. However, when tested alone, REGN10933, REGN10987, LY-CoV555,
106 LV-CoV016, CT-P59 and SARS2-38 completely lost neutralizing activity against B.1.1.529,
107 with little inhibitory capacity even at the highest (10,000 ng/mL) concentration tested. COV2-
108 and COV2-2196 showed an intermediate ~12 to 150-fold ($P < 0.0001$) loss in inhibitory
109 activity, respectively against the B.1.1.529 strain. In comparison, S309 showed a less than 2-fold
110 ($P > 0.5$) reduction in neutralizing activity against B.1.1.529 (**Fig 2a-h**). Analysis of mAb
111 combinations currently in clinical use showed that REGN10933/REGN10987 and LY-
112 CoV555/LV-CoV016 lost all neutralizing activity against B.1.1.529, whereas COV2-
113 2130/COV2-2196 showed a ~12-fold ($P < 0.0001$) reduction in inhibitory activity.

114 We repeated experiments in Vero-hACE2-TMPRSS2 cells to account for effects of
115 hACE2 expression, which can affect neutralization by some anti-SARS-CoV-2 mAbs^{19,22}.
116 Moreover, modeling studies suggest that the mutations in the B.1.1.529 spike may enhance
117 interactions with hACE2²³. All individual or combinations of mAbs tested neutralized the
118 WA1/2020 D614G isolate as expected. However, REGN10933, REGN10987, LY-CoV555, LV-
119 CoV016, SARS2-38, and CT-P59 completely lost neutralizing activity against B.1.1.529, and the

120 combinations of REGN10933/ REGN10987 or LY-CoV555/LV-CoV016 also lacked inhibitory
121 capacity (**Fig 3a-h**). In comparison, COV2-2196 showed moderately reduced activity (~16-fold)
122 as did the combination of COV2-2130/COV2-2196 mAbs (~11-fold). Unexpectedly, COV2-
123 2130 did not show a difference in neutralization of WA1/2020 and B.1.1.529 in the Vero-
124 hACE2-TMPRSS2 cells (**Fig 3a, g, and h**), whereas it did in Vero-TMPRSS2 cells (**Fig 2a, g,**
125 **and h**). The S309 mAb showed less potent neutralizing activity in Vero-hACE2-TMPRSS2 cells
126 at baseline with a flatter dose response curve (**Fig 3d**), as seen previously^{6,24}, and showed a
127 moderate (~6-fold, $P < 0.0001$) reduction in neutralizing activity against B.1.1.529 compared to
128 WA1/2020 D614G. Thus, while the trends in mAb neutralization of B.1.1.529 generally were
129 similar to Vero-TMPRSS2 cells, some expected and unexpected differences were noted with
130 COV2-2130 and S309 on cells expressing hACE2.

131 Our experiments show a marked loss of inhibitory activity by several of the most highly
132 neutralizing mAbs that are in advanced clinical development or have EUA approval. We
133 evaluated antibodies that correspond to monotherapy or combination therapy that have shown
134 pre- and post-exposure success in clinical trials and patients infected with historical SARS-CoV-
135 2 isolates. Our results confirm *in silico* predictions of how amino acid changes in B.1.1.529
136 RBD might negatively impact neutralizing antibody interactions^{16,25}. Moreover, they agree with
137 preliminary studies showing that several clinically used antibodies lose neutralizing activity
138 against B.1.1.529 spike-expressing recombinant lentiviral or vesicular stomatitis virus (VSV)-
139 based pseudoviruses²⁶⁻²⁸. One difference is that our study with authentic B.1.1.529 showed only
140 moderately reduced neutralization by antibodies corresponding to the AstraZeneca combination
141 (COV2-2196 and COV2-2130); in contrast, another group reported escape of these mAbs using a
142 VSV pseudovirus displaying a B.1.1.529 spike protein in Huh7 hepatoma cells²⁷. Additional

143 studies are needed to determine whether this disparity in results is due to the cell type, the virus
144 (authentic versus pseudotype), or preparation and combination of antibody.

145 While the Regeneron (REGN10933 and REGN10987), Lilly (LY-CoV555 and LV-
146 CoV016) and Celltrion (CT-P59) antibodies or combinations showed an almost complete loss of
147 neutralizing activity against B.1.1.529, in our assays with Vero-TMPRSS2 and Vero-hACE2-
148 TMPRSS2 cells, the mAbs corresponding to the AstraZeneca combination (COV-2196 and
149 COV-2130) or Vir Biotechnology (S309) products retained substantial inhibitory activity.
150 Although these data suggest that some of mAbs in clinical use may retain benefit, validation
151 experiments *in vivo*⁷ are needed to support this conclusion and inform clinical decisions.

152 Given the loss of inhibitory activity against B.1.1.529 of many highly neutralizing anti-
153 RBD mAbs in our study, it appears likely that serum polyclonal responses generated after
154 vaccination or natural infection also may lose substantial inhibitory activity against B.1.1.529,
155 which could compromise protective immunity and explain a rise in symptomatic infections in
156 vaccinated individuals²⁹. Indeed, studies have reported approximately 25 to 40-fold reductions in
157 serum neutralizing activity compared to historical D614G-containing strains from individuals
158 immunized with the Pfizer BNT162b2 and AstraZeneca AZD1222 vaccines^{26,28,30,31}.

159 We note several limitations of our study: (1) Our experiments focused on the impact of
160 the extensive sequence changes in the B.1.1.529 spike protein on mAb neutralization in cell
161 culture. Despite observing differences in neutralizing activity with certain mAbs, it remains to be
162 determined how this finding translates into effects on clinical protection against B.1.1.529; (2)
163 Although virus neutralization is a correlate of immune protection against SARS-CoV-2^{7,32,33}, this
164 measurement does not account for Fc effector functions if antibodies residually bind B.1.1.529
165 spike proteins on the virion or surface of infected cells. Fcγ receptor or complement protein

166 engagement by spike binding antibodies could confer substantial protection³⁴⁻³⁶; (3) We used the
167 prevailing B.1.1.529 Omicron isolate that lacks an R346K mutation. While only 8.3% of
168 B.1.1.529 sequences in GISAID (accessed on 12/14/2021) have an R346K mutation, this
169 substitution might negatively impact neutralization of some EUA mAbs given that it is a
170 crystallographic contact for COV2-2130, REGN10987, and S309 (**Fig 11**). At least for S309, the
171 R346K mutation did not impact neutralization of pseudoviruses displaying B.1.1.529 spike
172 proteins²⁸. Nonetheless, studies with infectious B.1.1.529 isolates with R346K mutations may be
173 warranted if the substitution becomes more prevalent; (4) Our data is derived from experiments
174 with Vero-TMPRSS2 and Vero-hACE2-TMPRSS2 cells. While these cells standardly are used
175 to measure antibody neutralization of SARS-CoV-2 strains, primary cells targeted by SARS-
176 CoV-2 *in vivo* can express unique sets of attachment and entry factors³⁷, which could impact
177 receptor and entry blockade by specific antibodies. Indeed, prior studies have reported that the
178 cell line used can affect the potency of antibody neutralization against different SARS-CoV-2
179 variants⁶.

180 In summary, our cell culture-based analysis of neutralizing mAb activity against an
181 authentic infectious B.1.1.529 Omicron SARS-CoV-2 isolate suggests that several, but not all,
182 existing therapeutic antibodies will lose protective benefit. Thus, the continued identification and
183 use of broadly and potently neutralizing mAbs that target the most highly conserved residues on
184 the SARS-CoV-2 spike likely is needed to prevent resistance against B.1.1.529 and future
185 variants with highly mutated spike sequences.

186

187 **ACKNOWLEDGEMENTS**

188 This study was supported by grants and contracts from NIH (R01 AI157155, U01
189 AI151810, 75N93021C00014, HHSN272201700060C, and 75N93019C00051), the Defense
190 Advanced Research Project Agency (HR0011-18-2-0001), the Japan Program for Infectious
191 Diseases Research and Infrastructure (JP21wm0125002) from the Japan Agency for Medical
192 Research and Development (AMED), and the Dolly Parton COVID-19 Research Fund at
193 Vanderbilt University Medical Center. We thank Rachel Nargi, Robert Carnahan, Tiong Tan,
194 and Lisa Schimanski for assistance and generosity with mAb generation and purification, and
195 Samuel A. Turner from the Center for Pathogen Evolution at the University of Cambridge for
196 evaluating B.1.1.529 sequences.

197

198 **AUTHOR CONTRIBUTIONS**

199 L.A.V. performed and analyzed neutralization assays. P.J.H. and L.A.V. propagated
200 SARS-CoV-2 viruses. P.H. performed sequencing analysis. J.E.C., S.J.Z., L.P., and D.C.
201 generated and provided mAbs. J.M.E. and D.H.F. performed structural analysis. J.E.C., Y.K.,
202 and M.S.D. obtained funding and supervised the research. L.A.V. and M.S.D. wrote the initial
203 draft, with all other authors providing editorial comments.

204

205 **COMPETING FINANCIAL INTERESTS**

206 M.S.D. is a consultant for Inbios, Vir Biotechnology, Senda Biosciences, and Carnival
207 Corporation, and on the Scientific Advisory Boards of Moderna and Immunome. The Diamond
208 laboratory has received funding support in sponsored research agreements from Moderna, Vir
209 Biotechnology, and Emergent BioSolutions. J.E.C. has served as a consultant for Luna Biologics

210 and Merck Sharp & Dohme Corp., is a member of the Scientific Advisory Boards of Meissa
211 Vaccines and is Founder of IDBiologics. The Crowe laboratory has received sponsored research
212 agreements from Takeda Vaccines, AstraZeneca and IDBiologics. Vanderbilt University has
213 applied for patents related to two antibodies in this paper. L.A.P. and D.C. are employees of Vir
214 Biotechnology and may hold equity in Vir Biotechnology. L.A.P is a former employee and
215 shareholder in Regeneron Pharmaceuticals.

216

217 **FIGURE LEGENDS**

218 **Figure 1. Neutralizing mAb epitopes on B.1.1.529. a-b**, SARS-CoV-2 spike trimer
219 (PDB: 7C2L and PDB: 6W41). One spike protomer is highlighted, showing the NTD in orange,
220 RBD in green, RBM in magenta, and S2 portion of the molecule in blue (**a**). Close-up view of
221 the RBD with the RBM outlined in magenta (**b**). Amino acids that are changed in B.1.1.529
222 compared to WA1/2020 are indicated in light green (**a-b**), with the exception of N679K and
223 P681H, which were not modeled in the structures used. **c-k**, SARS-CoV-2 RBD bound by EUA
224 mAbs COV2-2196 (**c**, PDB: 7L7D); COV2-2130 (**d**, PDB: 7L7E); S309 (**e**, PDB: 6WPS);
225 REGN-10987 (**f**, PDB: 6XDG); REGN-10933 (**g**, PDB: 6XDG)); LY-CoV555 (**h**, PDB: 7KMG)
226 LY-CoV016 (**i**, PDB: 7C01); CT-P59 (**j** PDB: 7CM4) and SARS2-38 (**k**, PDB: 7MKM).
227 Residues mutated in the B.1.1.529 RBD and contained in these mAbs respective epitopes are
228 shaded red, whereas those outside the epitope are shaded green. **l**, multiple sequence alignment
229 showing the epitope footprints of each EUA mAb on the SARS-CoV-2 RBD highlighted in cyan.
230 B.1.1.529 RBD is shown in the last row, with sequence changes relative to the WT RBD
231 highlighted red. A green diamond indicates the location of the N-linked glycan at residue 343.
232 Stars below the alignment indicate hACE2 contact residues on the SARS-CoV-2 RBD³⁸.

233 **Figure 2. Neutralization of SARS-CoV-2 B.1.1.529 Omicron strain by mAbs in**
234 **Vero-TMPRSS2 cells. a-f**, Neutralization curves in Vero-TMPRSS2 cells comparing the
235 sensitivity of SARS-CoV-2 strains with the indicated mAbs (COV2-2196, COV2-2130;
236 REGN10933, REGN10987, LY-CoV555, LY-CoV016, S309, CT-P59, and SARS2-38) with
237 WA1/2020 D614G and B.1.1.529. Also shown are the neutralization curves for antibody
238 cocktails (COV2-2196/COV2-2130, REGN10933/REGN10987, or LY-CoV555/LY-CoV016).
239 One representative experiment of three performed in technical duplicate is shown. Error bars

240 indicate range. **g**, Summary of EC₅₀ values (ng/ml) of neutralization of SARS-CoV-2 viruses
241 (WA1/2020 D614G and B.1.1.529) performed in Vero-TMPRSS2 cells. Data is the geometric
242 mean of 3 experiments. Blue shading: light, EC₅₀ > 5,000 ng/mL; dark, EC₅₀ > 10,000 ng/mL. **h**,
243 Comparison of EC₅₀ values by mAbs against WA1/2020 D614G and B.1.1.529 (3 experiments,
244 ns, not significant; ****, $P < 0.0001$; two-way ANOVA with Sidak's post-test). Bars indicate
245 mean values. The dotted line indicates the upper limit of dosing of the assay.

246 **Figure 3. Neutralization of SARS-CoV-2 B.1.1.529 Omicron strain by mAbs in**
247 **Vero-hACE2-TMPRSS2 cells. a-f**, Neutralization curves in Vero-hACE2-TMPRSS2 cells
248 comparing the sensitivity of SARS-CoV-2 strains with the indicated mAbs (S309, COV2-2196,
249 COV2-2130; REGN10933, REGN10987, LY-CoV555, LY-CoV016, CT-P59, and SARS2-38)
250 with WA1/2020 D614G and B.1.1.529. Also shown are the neutralization curves for antibody
251 cocktails (COV2-2196/COV2-2130, REGN10933/REGN10987, or LY-CoV555/LY-CoV016).
252 One representative experiment of three performed in technical duplicate is shown. Error bars
253 indicate range. **g**, Summary of EC₅₀ values (ng/ml) of neutralization of SARS-CoV-2 viruses
254 (WA1/2020 D614G and B.1.1.529) performed in Vero-hACE2-TMPRSS2 cells. Data is the
255 geometric mean of 3 experiments. Blue shading: light, EC₅₀ > 5,000 ng/mL; dark, EC₅₀ > 10,000
256 ng/mL. **h**, Comparison of EC₅₀ values by mAbs against WA1/2020 D614G and B.1.1.529 (3
257 experiments, ns, not significant; ****, $P < 0.0001$; two-way ANOVA with Sidak's post-test).
258 Bars indicate mean values. The dotted line indicates the upper limit of dosing of the assay.

259 **METHODS**

260 **Cells.** Vero-TMPRSS2³⁹ and Vero-hACE2-TMPRSS2⁶ cells were cultured at 37°C in
261 Dulbecco's Modified Eagle medium (DMEM) supplemented with 10% fetal bovine serum
262 (FBS), 10 mM HEPES pH 7.3, and 100 U/ml of penicillin–streptomycin. Vero-TMPRSS2
263 cells were supplemented with 5 µg/mL of blasticidin. Vero-hACE2-TMPRSS2 cells were
264 supplemented with 10 µg/mL of puromycin. All cells routinely tested negative for mycoplasma
265 using a PCR-based assay.

266 **Viruses.** The WA1/2020 recombinant strain with substitutions (D614G) was described
267 previously⁴⁰. The B.1.1.529 isolate (hCoV-19/USA/WI-WSLH-221686/2021) was obtained
268 from a midturbinate nasal swab and passaged once on Vero-TMPRSS2 cells as described⁴¹. All
269 viruses were subjected to next-generation sequencing (GISAID: EPI_ISL_7263803) to confirm
270 the stability of substitutions. All virus experiments were performed in an approved biosafety
271 level 3 (BSL-3) facility.

272 **Monoclonal antibody purification.** The mAbs used in this paper (COV2-2196, COV2-
273 2130, S309, REGN10933, REGN10987, LY-CoV555, LY-CoV016, CT-P59, SARS2-38) have
274 been described previously^{12,15,19,42-46}. COV2-2196 and COV2-2130 mAbs were produced after
275 transient transfection using the Gibco ExpiCHO Expression System (ThermoFisher Scientific)
276 following the manufacturer's protocol. Culture supernatants were purified using HiTrap
277 MabSelect SuRe columns (Cytiva, formerly GE Healthcare Life Sciences) on an AKTA Pure
278 chromatographer (GE Healthcare Life Sciences). Purified mAbs were buffer-exchanged into
279 PBS, concentrated using Amicon Ultra-4 50-kDa centrifugal filter units (Millipore Sigma) and
280 stored at -80°C until use. Purified mAbs were tested for endotoxin levels (found to be less than
281 30 EU per mg IgG). Endotoxin testing was performed using the PTS201F cartridge (Charles

282 River), with a sensitivity range from 10 to 0.1 EU per mL, and an Endosafe Nexgen-MCS
283 instrument (Charles River). S309, REGN10933, REGN10987, LY-CoV016, LY-CoV555, CT-
284 P59, and SARS2-38 mAb proteins were produced in CHOEXPI or EXPI293F cells and affinity
285 purified using HiTrap Protein A columns (GE Healthcare, HiTrap mAb select Xtra #28-4082-
286 61). Purified mAbs were suspended into 20 mM histidine, 8% sucrose, pH 6.0 or PBS. The final
287 products were sterilized by filtration through 0.22 μ m filters and stored at 4°C.

288 **Focus reduction neutralization test.** Serial dilutions of mAbs were incubated with 10²
289 focus-forming units (FFU) of SARS-CoV-2 (WA1/2020 D614G or B.1.1.529) for 1 h at 37°C.
290 Antibody-virus complexes were added to Vero-TMPRSS2 or Vero-hACE2-TMPRSS2 cell
291 monolayers in 96-well plates and incubated at 37°C for 1 h. Subsequently, cells were overlaid
292 with 1% (w/v) methylcellulose in MEM. Plates were harvested at 30 h (WA1/2020 D614G on
293 Vero-TMPRSS2 cells), 70 h (B.1.1.529 on Vero-TMPRSS2 cells), or 24 h (both viruses on
294 Vero-hACE2-TMPRSS2 cells) later by removal of overlays and fixation with 4% PFA in PBS
295 for 20 min at room temperature. Plates with WA1/2020 D614G were washed and sequentially
296 incubated with an oligoclonal pool of SARS2-2, SARS2-11, SARS2-16, SARS2-31, SARS2-38,
297 SARS2-57, and SARS2-71⁴⁷ anti-S antibodies. Plates with B.1.1.529 were additionally incubated
298 with a pool of mAbs that cross-react with SARS-CoV-1 and bind a CR3022-competing epitope
299 on the RBD¹⁹. All plates were subsequently stained with HRP-conjugated goat anti-mouse IgG
300 (Sigma, A8924) in PBS supplemented with 0.1% saponin and 0.1% bovine serum albumin.
301 SARS-CoV-2-infected cell foci were visualized using TrueBlue peroxidase substrate (KPL) and
302 quantitated on an ImmunoSpot microanalyzer (Cellular Technologies). Antibody-dose response
303 curves were analyzed using non-linear regression analysis with a variable slope (GraphPad
304 Software), and the half-maximal inhibitory concentration (EC₅₀) was calculated.

305 **Model of mAb-B.1.1.529 spike complexes.** The spike model is a composite of data from
306 PDB: 7C2L and PDB: 6W41. Models of mAb complexes were generated from their respective
307 PDB files with the following accession codes: COV2-2196 (PDB: 7L7D); COV2-2130 (PDB:
308 7L7E); S309 (PDB: 6WPS); REGN-10987 (PDB: 6XDG); REGN-10933 (PDB: 6XDG)); LY-
309 CoV555 (PDB: 7KMG) LY-CoV016 (PDB: 7C01); CT-P59 (PDB: 7CM4) and SARS2-38
310 (PDB: 7MKM). Epitope footprints used in the multiple sequence alignment were determined
311 using PISA interfacial analysis on the various mAb:RBD complexes⁴⁸. Structural figures were
312 generated using UCSF ChimeraX⁴⁹.

313 **Data availability.** All data supporting the findings of this study are available within the
314 paper and are available from the corresponding author upon request.

315 **Code availability.** No code was used in the course of the data acquisition or analysis.

316 **Reagent availability.** All reagents described in this paper are available through Material
317 Transfer Agreements.

318 **Statistical analysis.** The number of independent experiments and technical replicates
319 used are indicated in the relevant Figure legends. A two-way ANOVA with Sidak's post-test was
320 used for comparisons of antibody potency between WA1/2020 D614G and B.1.1.59.

321

322

323 **REFERENCES**

324

325 1. Sempowski, G.D., Saunders, K.O., Acharya, P., Wiehe, K.J. & Haynes, B.F. Pandemic
326 Preparedness: Developing Vaccines and Therapeutic Antibodies For COVID-19. *Cell*
327 **181**, 1458-1463 (2020).

328 2. Wibmer, C.K., *et al.* SARS-CoV-2 501Y.V2 escapes neutralization by South African
329 COVID-19 donor plasma. *bioRxiv* (2021).

330 3. Wang, Z., *et al.* mRNA vaccine-elicited antibodies to SARS-CoV-2 and circulating
331 variants. *Nature* (2021).

332 4. Tada, T., *et al.* Neutralization of viruses with European, South African, and United States
333 SARS-CoV-2 variant spike proteins by convalescent sera and BNT162b2 mRNA
334 vaccine-elicited antibodies. *bioRxiv* (2021).

335 5. Wang, P., *et al.* Antibody Resistance of SARS-CoV-2 Variants B.1.351 and B.1.1.7.
336 *Nature* (2021).

337 6. Chen, R.E., *et al.* Resistance of SARS-CoV-2 variants to neutralization by monoclonal
338 and serum-derived polyclonal antibodies. *Nat Med* (2021).

339 7. Chen, R.E., *et al.* In vivo monoclonal antibody efficacy against SARS-CoV-2 variant
340 strains. *Nature* (2021).

341 8. Callaway, E. & Ledford, H. How bad is Omicron? What scientists know so far. *Nature*
342 (2021).

343 9. Torjesen, I. Covid-19: Omicron may be more transmissible than other variants and partly
344 resistant to existing vaccines, scientists fear. *BMJ (Clinical research ed* **375**, n2943
345 (2021).

346 10. Johnson, B.A., *et al.* Loss of furin cleavage site attenuates SARS-CoV-2 pathogenesis.
347 *Nature* (2021).

348 11. Chen, J., Wang, R., Gilby, N.B. & Wei, G.W. Omicron (B.1.1.529): Infectivity, vaccine
349 breakthrough, and antibody resistance. *ArXiv* (2021).

350 12. Pinto, D., *et al.* Cross-neutralization of SARS-CoV-2 by a human monoclonal SARS-
351 CoV antibody. *Nature* **583**, 290-295 (2020).

352 13. Gupta, A., *et al.* Early Treatment for Covid-19 with SARS-CoV-2 Neutralizing Antibody
353 Sotrovimab. *N Engl J Med* **385**, 1941-1950 (2021).

354 14. Zost, S.J., *et al.* Potently neutralizing and protective human antibodies against SARS-
355 CoV-2. *Nature* **584**, 443-449 (2020).

356 15. Baum, A., *et al.* REGN-COV2 antibodies prevent and treat SARS-CoV-2 infection in
357 rhesus macaques and hamsters. *Science* (2020).

358 16. Starr, T.N., Greaney, A.J., Dingens, A.S. & Bloom, J.D. Complete map of SARS-CoV-2
359 RBD mutations that escape the monoclonal antibody LY-CoV555 and its cocktail with
360 LY-CoV016. *Cell reports. Medicine*, 100255 (2021).

361 17. Gottlieb, R.L., *et al.* Effect of Bamlanivimab as Monotherapy or in Combination With
362 Etesevimab on Viral Load in Patients With Mild to Moderate COVID-19: A Randomized
363 Clinical Trial. *Jama* **325**, 632-644 (2021).

364 18. Kim, C., *et al.* A therapeutic neutralizing antibody targeting receptor binding domain of
365 SARS-CoV-2 spike protein. *Nat Commun* **12**, 288 (2021).

366 19. VanBlargan, L.A., *et al.* A potently neutralizing SARS-CoV-2 antibody inhibits variants
367 of concern by utilizing unique binding residues in a highly conserved epitope. *Immunity*
368 (2021).

369 20. Case, J.B., *et al.* Neutralizing antibody and soluble ACE2 inhibition of a replication-
370 competent VSV-SARS-CoV-2 and a clinical isolate of SARS-CoV-2. *Cell Host and*
371 *Microbe* **28**, 475-485 (2020).

372 21. Cathcart, A.L., *et al.* The dual function monoclonal antibodies VIR-7831 and VIR-7832
373 demonstrate potent *in vitro* and *in vivo* activity against SARS-CoV-2. *bioRxiv*,
374 2021.2003.2009.434607 (2021).

375 22. Suryadevara, N., *et al.* Neutralizing and protective human monoclonal antibodies
376 recognizing the N-terminal domain of the SARS-CoV-2 spike protein. *Cell* **184**, 2316-
377 2331.e2315 (2021).

378 23. Golcuk, M., Yildiz, A. & Gur, M. The Omicron Variant Increases the Interactions of
379 SARS-CoV-2 Spike Glycoprotein with ACE2. *bioRxiv*, 2021.2012.2006.471377 (2021).

380 24. Lempp, F.A., *et al.* Lectins enhance SARS-CoV-2 infection and influence neutralizing
381 antibodies. *Nature* **598**, 342-347 (2021).

382 25. Ford, C.T., Machado, D.J. & Janies, D.A. Predictions of the SARS-CoV-2 Omicron
383 Variant (B.1.1.529) Spike Protein Receptor-Binding Domain Structure and Neutralizing
384 Antibody Interactions. *bioRxiv*, 2021.2012.2003.471024 (2021).

385 26. Wilhelm, A., *et al.* Reduced Neutralization of SARS-CoV-2 Omicron Variant by Vaccine
386 Sera and monoclonal antibodies. *medRxiv : the preprint server for health sciences*,
387 2021.2012.2007.21267432 (2021).

388 27. Cao, Y.R., *et al.* B.1.1.529 escapes the majority of SARS-CoV-2 neutralizing antibodies
389 of diverse epitopes. *bioRxiv*, 2021.2012.2007.470392 (2021).

390 28. Cameroni, E., *et al.* Broadly neutralizing antibodies overcome SARS-CoV-2 Omicron
391 antigenic shift. *bioRxiv*, 2021.2012.2012.472269 (2021).

392 29. Callaway, E. Omicron likely to weaken COVID vaccine protection. *Nature* (2021).

393 30. Cele, S., *et al.* SARS-CoV-2 Omicron has extensive but incomplete escape of Pfizer
394 BNT162b2 elicited neutralization and requires ACE2 for infection. *medRxiv : the*
395 *preprint server for health sciences*, 2021.2012.2008.21267417 (2021).

396 31. Dejnirattisai, W., *et al.* Reduced neutralisation of SARS-CoV-2 Omicron-B.1.1.529
397 variant by post-immunisation serum. *medRxiv : the preprint server for health sciences*,
398 2021.2012.2010.21267534 (2021).

399 32. Kim, J.H., Marks, F. & Clemens, J.D. Looking beyond COVID-19 vaccine phase 3 trials.
400 *Nat Med* (2021).

401 33. Khoury, D.S., *et al.* Neutralizing antibody levels are highly predictive of immune
402 protection from symptomatic SARS-CoV-2 infection. *Nat Med* **27**, 1205-1211 (2021).

403 34. Schäfer, A., *et al.* Antibody potency, effector function, and combinations in protection
404 and therapy for SARS-CoV-2 infection *in vivo*. *J Exp Med* **218**(2021).

405 35. Zohar, T., *et al.* Compromised Humoral Functional Evolution Tracks with SARS-CoV-2
406 Mortality. *Cell* **183**, 1508-1519.e1512 (2020).

407 36. Winkler, E.S., *et al.* Human neutralizing antibodies against SARS-CoV-2 require intact
408 Fc effector functions for optimal therapeutic protection. *Cell* **184**, 1804-1820.e1816
409 (2021).

410 37. Bailey, A.L. & Diamond, M.S. A Crisp(r) New Perspective on SARS-CoV-2 Biology.
411 *Cell* **184**, 15-17 (2021).

412 38. Lan, J., *et al.* Structure of the SARS-CoV-2 spike receptor-binding domain bound to the
413 ACE2 receptor. *Nature* **581**, 215-220 (2020).

414 39. Zang, R., *et al.* TMPRSS2 and TMPRSS4 promote SARS-CoV-2 infection of human
415 small intestinal enterocytes. *Sci Immunol* **5**(2020).

416 40. Plante, J.A., *et al.* Spike mutation D614G alters SARS-CoV-2 fitness. *Nature* (2020).

417 41. Imai, M., *et al.* Syrian hamsters as a small animal model for SARS-CoV-2 infection and
418 countermeasure development. *Proc Natl Acad Sci U S A* **117**, 16587-16595 (2020).

419 42. Zost, S.J., *et al.* Rapid isolation and profiling of a diverse panel of human monoclonal
420 antibodies targeting the SARS-CoV-2 spike protein. *Nat Med* **26**, 1422-1427 (2020).

421 43. Tortorici, M.A., *et al.* Ultrapotent human antibodies protect against SARS-CoV-2
422 challenge via multiple mechanisms. *Science* **370**, 950-957 (2020).

423 44. Baum, A., *et al.* Antibody cocktail to SARS-CoV-2 spike protein prevents rapid
424 mutational escape seen with individual antibodies. *Science* (2020).

425 45. Jones, B.E., *et al.* LY-CoV555, a rapidly isolated potent neutralizing antibody, provides
426 protection in a non-human primate model of SARS-CoV-2 infection. *bioRxiv* (2020).

427 46. Shi, R., *et al.* A human neutralizing antibody targets the receptor-binding site of SARS-
428 CoV-2. *Nature* **584**, 120-124 (2020).

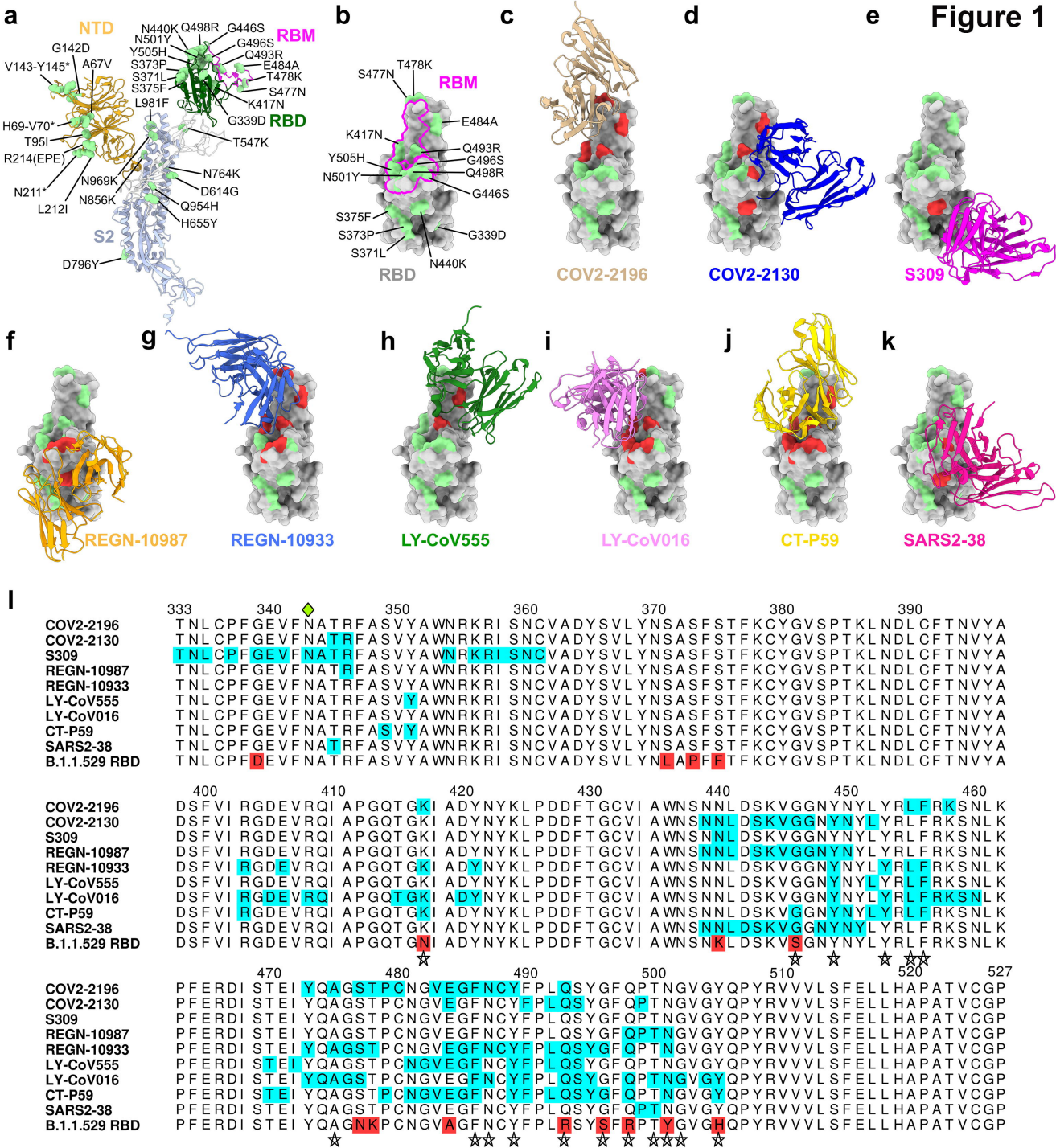
429 47. Liu, Z., *et al.* Identification of SARS-CoV-2 spike mutations that attenuate monoclonal
430 and serum antibody neutralization. *Cell Host Microbe* **29**, 477-488.e474 (2021).

431 48. Krissinel, E. & Henrick, K. Inference of macromolecular assemblies from crystalline
432 state. *J Mol Biol* **372**, 774-797 (2007).

433 49. Goddard, T.D., *et al.* UCSF ChimeraX: Meeting modern challenges in visualization and
434 analysis. *Protein Sci* **27**, 14-25 (2018).

435

Figure 1



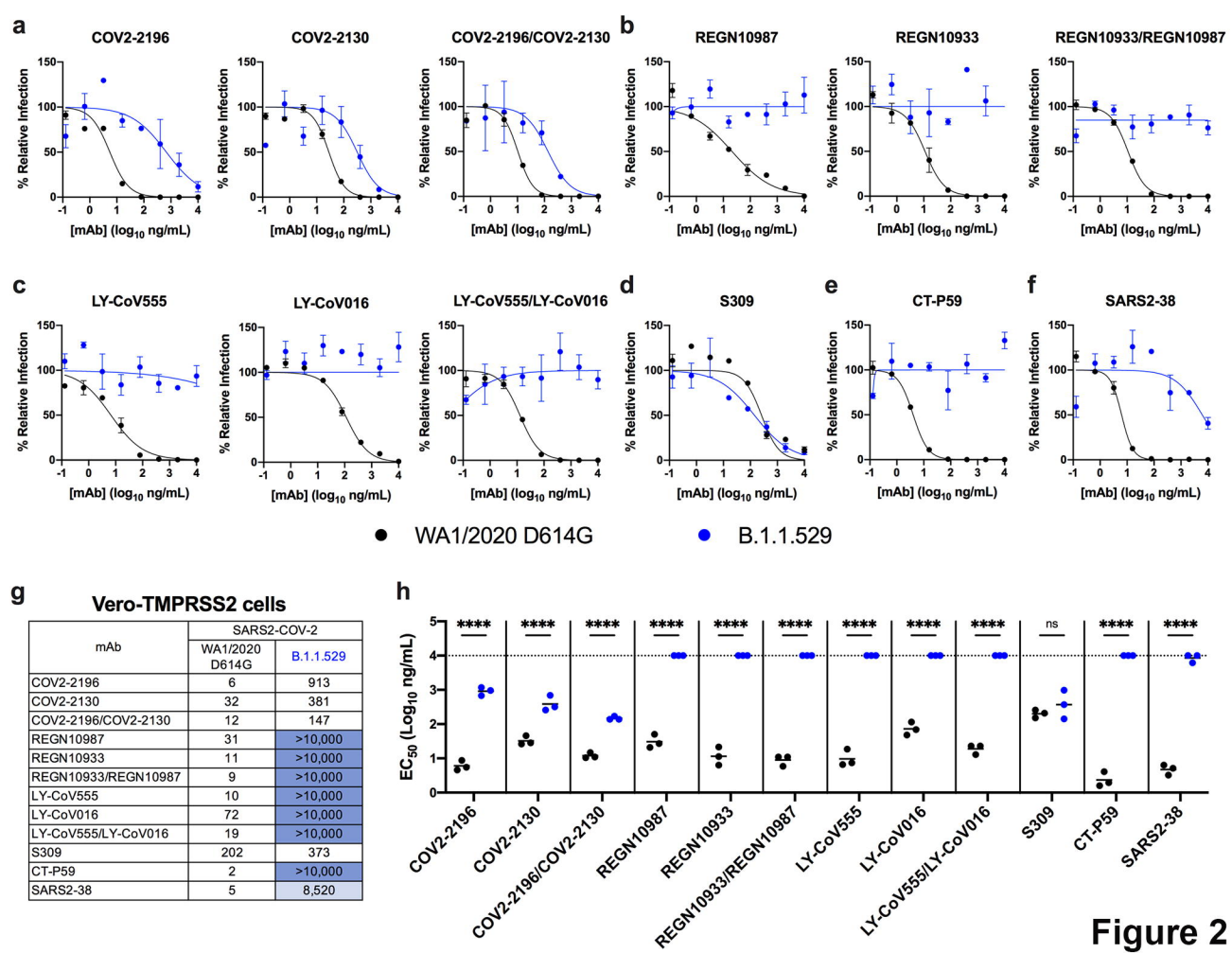


Figure 2

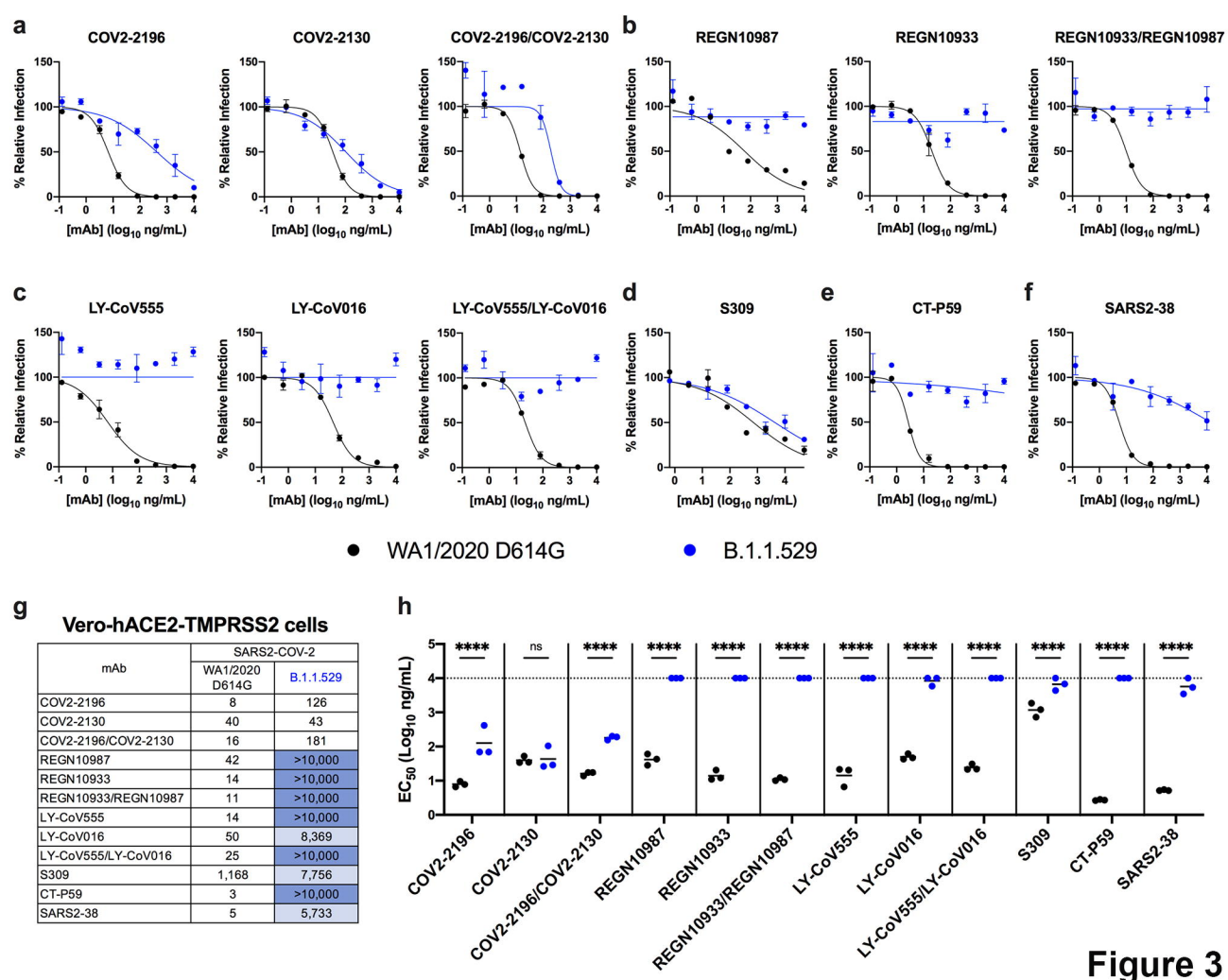


Figure 3